


 Cite this: *RSC Adv.*, 2024, 14, 25802

# Fabrication and characterization of a chitosan/cyclodextrin/TiO<sub>2</sub>-NPs composite for preservation of avocados

 Thi Lan Pham,<sup>ID</sup>\*<sup>ab</sup> Manh B. Nguyen,<sup>ID</sup><sup>c</sup> Van Cuong Bui,<sup>a</sup> Thi Xuyen Nguyen,<sup>ab</sup> Savitskaya T. A.,<sup>d</sup> Irina Le-Deygen,<sup>e</sup> Hoang Thai<sup>a</sup> and Dai Lam Tran<sup>a</sup>

In this study, a TiO<sub>2</sub> material with nanoparticle size of about 10–20 nm, surface area of 109 m<sup>2</sup> g<sup>-1</sup> was synthesized using the microwave-assisted hydrothermal method. The chitosan/TiO<sub>2</sub> film combined with cyclodextrin (chitosan–cyclodextrin/TiO<sub>2</sub>, CS–CD/TiO<sub>2</sub>NPs) helps significantly improve the mechanical properties and enhance the antibacterial activity of the polymer film. Furthermore, the content of TiO<sub>2</sub> nanoparticles in CS–CD/TiO<sub>2</sub>NPs also affects the tensile strength, antibacterial activity, ripening rate, ethylene production rate, and water vapor permeability during food preservation of the CS–CD film that has been studied. The CS–CD/TiO<sub>2</sub>NPs film is effective against Gram-negative bacteria (*Escherichia coli*) and Gram-positive bacteria (*Staphylococcus aureus*) reaching over 99.5% after 15 min of contact. The preservation ability of avocados coated with CS–CD/TiO<sub>2</sub>NPs was evaluated through some physiological parameters of the avocados, such as sensory evaluation, weight loss, and hardness. The results show that the use of CS–CD/TiO<sub>2</sub>NPs films extends the preservation time of avocados up to 7 days under conditions of 30 °C and 80% relative humidity.

 Received 10th June 2024  
 Accepted 9th August 2024

DOI: 10.1039/d4ra04207g

[rsc.li/rsc-advances](http://rsc.li/rsc-advances)

## 1 Introduction

Many fruits, such as mangoes, bananas, and avocados, contain essential nutrients for humans, such as minerals, fiber, and vitamins.<sup>1</sup> However, these foods are prone to spoilage during transportation and storage, as they can be attacked by microorganisms, that convert nutrients into harmful substances.<sup>2</sup> Therefore, generations of food preservation materials have been developed, with the most common being food films made from polymers derived from petroleum products.<sup>3</sup> The process of wrapping food with these films can be affected by temperature and can permeate the food, posing health risks. Additionally, the polymers currently used have low biodegradability, high toxicity, and contribute to the serious plastic pollution crisis.<sup>4</sup> Therefore, biodegradable food preservation films that are environmentally friendly and have high mechanical strength have been developed to extend the shelf life of food.<sup>5–7</sup> Ultra-thin biological film materials coated on the surface of food will

provide a barrier for water vapor, CO<sub>2</sub>, oxygen, and the transport of soluble substances for the food.<sup>8</sup> These coatings can be applied to the food surface very simply, including by immersion, spraying, or direct brushing to create semi-permeable film layers on the food surface, helping reduce respiration, water loss, and moisture control. Edible coatings have been used for a long time to maintain the quality and extend the shelf life of some fresh fruits, such as oranges, lemons, limes, apples, cucumbers, *etc.*<sup>9–11</sup> Some polysaccharides have been used as food preservation coatings, such as starch, pectin, cellulose, and alginate.<sup>12</sup> Recently, chitosan (CS) film has been considered a material that can replace traditional preservation membrane materials because it is cost-effective, abundant in supply, biocompatible, highly biodegradable, antimicrobial, non-toxic, environmentally friendly, and highly renewable, and originates from crustacean shells.<sup>13–15</sup>

Furthermore, chitosan film has high mechanical strength, can adjust moisture and air permeability easily, thus extending its shelf life even in harsh conditions. However, very thin chitosan films may affect biological activity and antimicrobial properties, so the addition of additives to enhance mechanical properties, antioxidant ability, antimicrobial, and antifungal properties is essential. To enhance water and gas vapor resistance, and improve mechanical properties such as tensile strength and thermal stability, nanoparticles such as ZnO or TiO<sub>2</sub> have been used as additives.<sup>13</sup> Motelica *et al.*<sup>16</sup> used a chitosan/ZnO/Ag NP/lemongrass essential oil film as a biodegradable antibacterial coating for grapes. The chitosan/ZnO/Ag NP/

<sup>a</sup>Institute for Tropical Technology, Vietnam Academy of Science and Technology, 18 Hoang Quoc Viet, Cau Giay, Hanoi, Vietnam. E-mail: [ptlan@itt.vast.vn](mailto:ptlan@itt.vast.vn)

<sup>b</sup>Graduate University of Science and Technology, Vietnam Academy of Science and Technology, 18 Hoang Quoc Viet, Cau Giay, Hanoi, Vietnam

<sup>c</sup>Institute of Chemistry, Vietnam Academy of Science and Technology, 18 Hoang Quoc Viet, Cau Giay, Hanoi, Vietnam

<sup>d</sup>Research Institute for Physical Chemical Problems, Belarusian State University, Minsk, Belarus

<sup>e</sup>Chemical Enzymology Department, Lomonosov Moscow State University, Leninskie Gory 11b, Moscow, Russian Federation



lemongrass essential oil film showed antibacterial properties against Gram-positive bacteria, Gram-negative bacteria, and fungi. After 14 days of storage with the chitosan/ZnO/Ag NP/lemongrass essential oil film, the grapes only had a few rust spots and showed no signs of spoilage.

Titanium dioxide nanoparticles (TiO<sub>2</sub>-NPs) are non-toxic, have high chemical stability, a low production cost, and antimicrobial properties.<sup>17–19</sup> Especially under semiconductor light conditions, TiO<sub>2</sub> can be self-activated to form reactive oxygen species such as hydroxyl (<sup>•</sup>OH) and superoxide (<sup>•</sup>O<sub>2</sub><sup>−</sup>) radicals.<sup>20,21</sup> These reaction radicals can combine with unsaturated phospholipids on membrane layers to eliminate pathogens.<sup>22</sup> Indeed, Wang *et al.* reported that the <sup>•</sup>OH and <sup>•</sup>O<sub>2</sub><sup>−</sup> radicals are the main reactive oxygen species (ROS) that antibacterial *E. coli*.<sup>23</sup> TiO<sub>2</sub> nanoparticles can disrupt cell walls and film to degrade bacteria, showing antibacterial effects, and can degrade ethylene released during the preservation of fruits and vegetables into water and CO<sub>2</sub>.<sup>24</sup> Cho *et al.*<sup>24</sup> used a nano-TiO<sub>2</sub>/UV photocatalyst to disinfect bacteria on carrot surfaces and found that the shelf life of carrots was significantly extended. Xing *et al.*<sup>25</sup> found that nano-TiO<sub>2</sub> can inhibit bacteria such as *Penicillium digitatum*, and *Escherichia coli* parasitizing on citrus fruits, helping the fruits stay fresher. Furthermore, chitosan/TiO<sub>2</sub> film is applied as a material for adsorbing metal ions and antibiotics in water. The chitosan/TiO<sub>2</sub> film can adsorb 297 and 315 mg g<sup>−1</sup> of Pb<sup>2+</sup> and Cd<sup>2+</sup> ions respectively, and efficiently degrade various antibiotics such as tetracycline (98%), meropenem (98%), vancomycin (86%), and erythromycin (88%). Additionally, the chitosan/TiO<sub>2</sub> film has effective antibacterial properties against *Escherichia coli*, *Citrobacter* spp, *Enterococcus faecalis* and *Staphylococcus aureus*.<sup>26</sup> However, chitosan combined with nanoparticle TiO<sub>2</sub> additives often easily agglomerates and can reduce the mechanical properties of the chitosan membrane as the nanoparticles are unevenly distributed on the coating layer.<sup>27</sup> To overcome this drawback, Du *et al.*<sup>28</sup> combined nanoparticles with β-cyclodextrin through the hydroxyl groups on the outer edge of the molecule to effectively preserve strawberries and tomatoes. Studies have confirmed that the addition of CD significantly improves the antibacterial activity as well as the mechanical properties of the polymer membrane.<sup>29–31</sup>

The most common food preservation materials nowadays originate from petroleum products, with low biodegradability, high toxicity, and the ability to permeate into food, posing risks to health. For biofilms, the combination of chitosan (CS) with nanoparticles (NPs) often leads to uneven distribution of NPs on the coating layer, resulting in aggregation and reduction of the mechanical properties of the chitosan film. The aim of this study is to successfully synthesize a chitosan film with antibacterial properties, high mechanical strength, and biodegradability for use as packaging material to extend the shelf life of avocados, a nutritious and popular fruit in Vietnam. In addition, currently, the types of films used to preserve avocados are very limited, with low effectiveness, and the films have poor biodegradability. To overcome the drawbacks of TiO<sub>2</sub> nanoparticles easily aggregating when combined with chitosan, reducing the mechanical properties of the chitosan/TiO<sub>2</sub> film. In this study, we used hydroxyl groups of β-cyclodextrin to significantly improve the antibacterial activity and mechanical

properties of the CS-CD/TiO<sub>2</sub>NPs film. To our knowledge, this is the first study to combine TiO<sub>2</sub> nanoparticles simultaneously with chitosan and CS-based film. The coating layer based on chitosan with CD and TiO<sub>2</sub> nanoparticles (referred to as CS-CD/TiO<sub>2</sub>NPs coating layer) was fabricated from TiO<sub>2</sub> nanoparticles with sizes ranging from 10–20 nm using a microwave-assisted hydrothermal method. The content of TiO<sub>2</sub> nanoparticles affects the tensile strength, antibacterial activity, and avocado preservation ability, which were evaluated through various physiological parameters of avocados, such as sensory evaluation, weight loss, and hardness.

## 2 Materials and methods

The *Persea americana* Mill avocados variety reaches maturity for harvesting, with dark green fruit skin, weighing about 250 g per fruit, firmness of 1.6 N, dry weight of 20.31%; lipid content of 12.25% harvested in Dak Mil district, Dak Nong, Vietnam. Titanium(IV) isopropoxide (TTIP, 97%), acetic acid (98%), chitosan (CS, 99.9%, white powder, deacetylation degree 83.7%, molecular weight 82 kDa), and hydroxypropyl-β-cyclodextrin (HPβCD) were purchased from Sigma-Aldrich.

### 2.1. Synthesis of TiO<sub>2</sub> nanoparticles

TiO<sub>2</sub> sample is synthesized using the microwave-assisted hydrothermal method. Specifically, 2.28 mL of titanium(IV) isopropoxide (TTIP) is added to a mixture of 80 mL of ethanol and acetic acid (1 : 1) and vigorously stirred to form a homogeneous mixture, then added to the Teflon reaction vial. This mixture is crystallized using the microwave-assisted hydrothermal method in a microwave device (power 700 W) for 30 minutes at a temperature of 100 °C.<sup>17</sup> The white solid is separated by centrifugation and washed three times with distilled water to remove any unreacted substances. Next, the product is dried for 12 hours at 80 °C and finely ground using a mortar and pestle before being heated at 450 °C for 4 hours to obtain TiO<sub>2</sub> nanoparticles.

### 2.2. Synthesis of chitosan/cyclodextrin-TiO<sub>2</sub>NPs (CS-CD/TiO<sub>2</sub>NPs)

Based on our previous research, the concentration of 1.5% chitosan solution was chosen for this study.<sup>32</sup> First, 1.5 g of CS was dissolved in 100 mL of 1% acetic acid solution, then 0.1 g of HP-β-CD was added to the mixture and stirred at 40 °C for 2 hours to obtain a 1.6 mg per mL CS-CD solution. At the same time, 1 g of TiO<sub>2</sub> is added to 10 mL of distilled water and sonicated for 30 minutes to obtain a homogeneous suspension. Next, 16 μL of TiO<sub>2</sub> suspension is added to 10 mL of the CS-CD solution and stirred at room temperature for 4 hours to obtain a homogeneous emulsion. This solution is then placed in a Petri dish and allowed to dry naturally, resulting in a CS-CD/1% TiO<sub>2</sub>NPs material. The TiO<sub>2</sub> content in the CS-CD film is investigated by adding 8, 16, 24, and 32 μL of the TiO<sub>2</sub> solution (100 mg mL<sup>−1</sup>) to 10 mL of the CS-CD solution, resulting in CS-CD/0.5%TiO<sub>2</sub>, CS-CD/1%TiO<sub>2</sub>, and CS-CD/1.5%TiO<sub>2</sub> and CS-CD/2%TiO<sub>2</sub> coatings, respectively.



### 2.3. Characterization of TiO<sub>2</sub> nanoparticles and CS-CD/TiO<sub>2</sub>NPs coatings

X-ray diffraction (XRD) is measured using the D8 Advance X-ray diffractometer (Bruker, Germany) with a CuK<sub>α</sub> radiation source ( $2\theta$  range of 10–80° and  $\lambda = 0.15406$  nm). The morphology of the TiO<sub>2</sub> and CS-CD/TiO<sub>2</sub>NPs samples was examined by transmission electron microscopy (TEM) with an acceleration voltage of 200 kV (Leica IEO 906E). FT-IR is measured using the Jasco 4700 spectrophotometer. The sample surface area is measured on the Tristar-3030 system (Micromeritics-USA) with N<sub>2</sub> adsorption at 77 K using the BET method. The TiO<sub>2</sub> material was degas at 200 °C for 5 hours in a vacuum environment to clean the material surface before being introduced into the Tristar-3030 system.<sup>33</sup> The CS-CD and CS-CD/TiO<sub>2</sub> materials with dimensions of 10 × 50 mm are tested for tensile strength using the GOTECH AI-7000M universal mechanical testing machine, following ASTM D882 standard.

### 2.4. Evaluation of the antibacterial activity of the films-forming product

In this study, products with different compositions of CS-CD/TiO<sub>2</sub> were tested for their antibacterial ability against two bacterial strains, *Escherichia coli* and *Staphylococcus aureus*. *Escherichia coli* and *Staphylococcus aureus* bacteria are two types of bacteria representing negative and positive gram that are

harmful to humans and food during preservation.<sup>28</sup> The microbes were exposed to the material to evaluate resistance index, with a concentration of 10<sup>4</sup> CFU mL<sup>-1</sup> for both *E. coli* and *Staphylococcus aureus*. Then, UV light was irradiated for 5 minutes, followed by a 10 min incubation period (the total material contact time was 15 minutes).<sup>28</sup> The control sample, without the addition of material, only had a tested microorganism density of 10<sup>4</sup> CFU mL<sup>-1</sup>. The spread plate method was used to determine the microorganism concentration after the experiment.

### 2.5. Evaluating some of physiological parameters

**2.5.1 Process of creating film on avocados.** After being cleaned and dried in the air, the avocados are immersed in the CS-CD/0.5%TiO<sub>2</sub> or CS-CD/1.0%TiO<sub>2</sub> mixture to form a protective coating. Then, the avocados are placed on a plastic tray for the coating to dry naturally at room temperature. Finally, the avocados are covered with a protective film to be stored at room temperature and to monitor the changes in the biochemical indices of the avocados at different times.<sup>32</sup>

**2.5.2 Mass loss analysis.** The mass of avocados is determined daily using an analytical balance with a weighing capacity ranging from 0.50 to 3200.00 g and a readability of 0.01 g. The difference in mass between each time interval during storage is considered the mass loss. The mass loss ( $L_m$ ) is

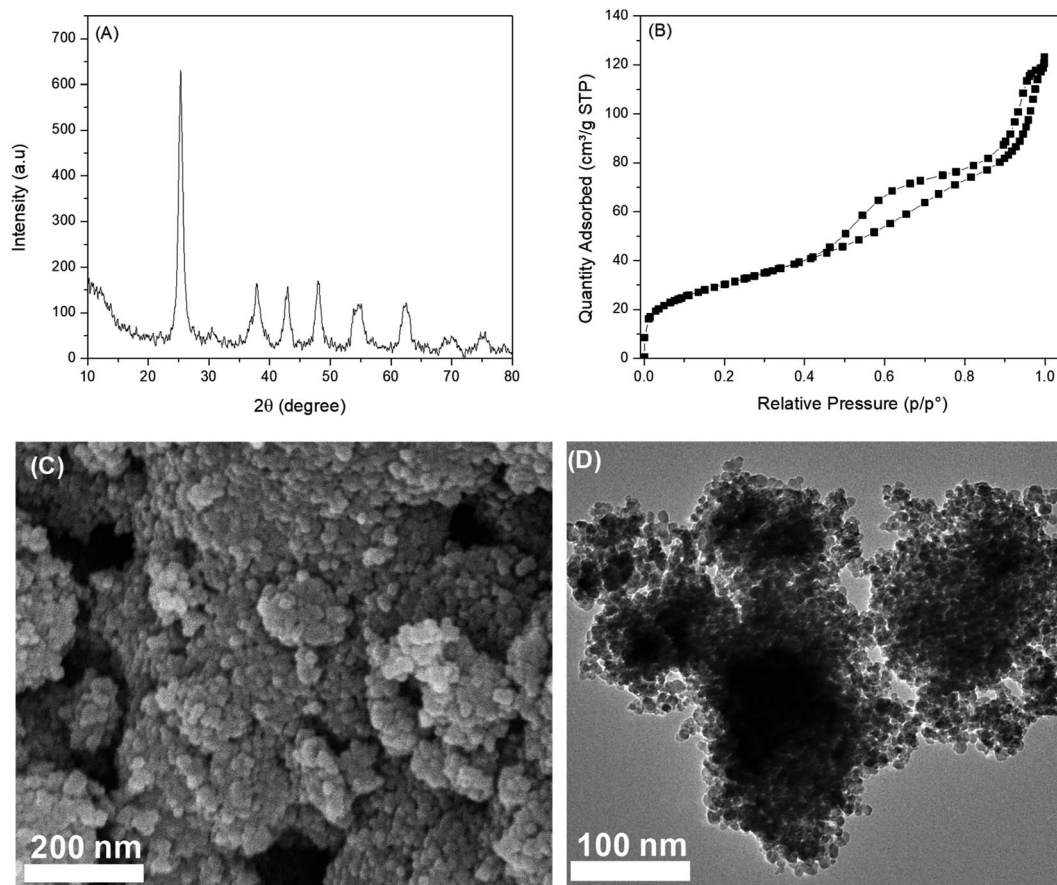


Fig. 1 (A) XRD pattern, (B) N<sub>2</sub> adsorption–desorption isotherm, (C) SEM image and (D) TEM image of TiO<sub>2</sub>NPs.



calculated as the percentage difference in weight according to formula (2). The weight measurements are repeated at least three times to ensure accuracy.<sup>32</sup>

$$L_m = \frac{m_0 - m}{m_0} \times 100\% \quad (1)$$

where  $m_0$  is initial fruit weight (g);  $m$  is fruit weight after days of preservation (g).

**2.5.3 Determination of the hardness.** The hardness of the fruits ( $X$ ) is calculated by the Fruit Hardness Tester FHM-5 device (Japan) based on the formula:

$$X (\text{kg cm}^{-2}) = \frac{F}{S} \quad (2)$$

where,  $X$  is a hardness of the fruit ( $\text{kg cm}^{-2}$ ),  $F$  is a force magnitude on the fruit (kg), and  $S$  is the contact area of the needle ( $\text{cm}^2$ ).

The result is presented as the average value of 3 repetitions of the experiment, with a sample size of 3 fruits per repetition. Each fruit is measured three times at three different positions on the fruit.

## 3 Results and discussion

### 3.1. Characterization of $\text{TiO}_2$ nanoparticles ( $\text{TiO}_2$ -NPs)

The structural properties, surface area, pore volume, and morphology of  $\text{TiO}_2$  are presented in Fig. 1. The  $\text{TiO}_2$ -NPs with peaks at  $2\theta$  of  $25.42^\circ$ ,  $37.83^\circ$ ,  $47.93^\circ$ ,  $54.12^\circ$ , and  $62.34^\circ$

correspond to the (101), (004), (200), (105), and (204) planes, respectively, in the anatase phase of  $\text{TiO}_2$  (JCPDS No. 89-4921).<sup>34,35</sup> In addition, the peak at  $2\theta$  of  $42.51^\circ$  assigned to the rutile phase of  $\text{TiO}_2$  (JCPDS No. 88-1175).<sup>36</sup> The average crystal size of the  $\text{TiO}_2$  nanomaterial is determined to be approximately 5 nm using the Debye–Scherrer equation. The Bragg's law and Miller indices are applied to determine the lattice parameters of the tetragonal phase structure of  $\text{TiO}_2$  ( $\alpha = \beta = \gamma = 90^\circ$ ,  $a = b = 3.786 \text{ \AA}$ ,  $c = 9.516 \text{ \AA}$ ).

The  $\text{N}_2$  adsorption–desorption isotherms of the  $\text{TiO}_2$  sample fall into the type IV category according to IUPAC, with a hysteresis loop in the relative pressure range of 0.45 to 0.1 (Fig. 1B).<sup>37</sup> The  $\text{TiO}_2$  material has a surface area, pore volume, and pore diameter of  $109 \text{ m}^2 \text{ g}^{-1}$ ,  $0.182 \text{ cm}^3 \text{ g}^{-1}$ , and 6.93 nm, respectively. The scanning electron microscopy (SEM) and TEM images of the  $\text{TiO}_2$  material show spherical nanoparticles with size of 10–20 nm, and the nanoparticle size is very uniform (Fig. 1C and D).

### 3.2. Characteristic properties of CS–CD/ $\text{TiO}_2$ NPs films

The SEM images of CS–CD/ $\text{TiO}_2$  films with different  $\text{TiO}_2$  contents are presented in Fig. 2. Fig. 2 confirms that the addition of  $\text{TiO}_2$  to the chitosan–cyclodextrin films affects the morphology of the film. When the  $\text{TiO}_2$  content increases from 0.5 to 2 wt%, the surface of the chitosan–cyclodextrin film shows more small particles, with particle sizes ranging from 10 to 20 nm.

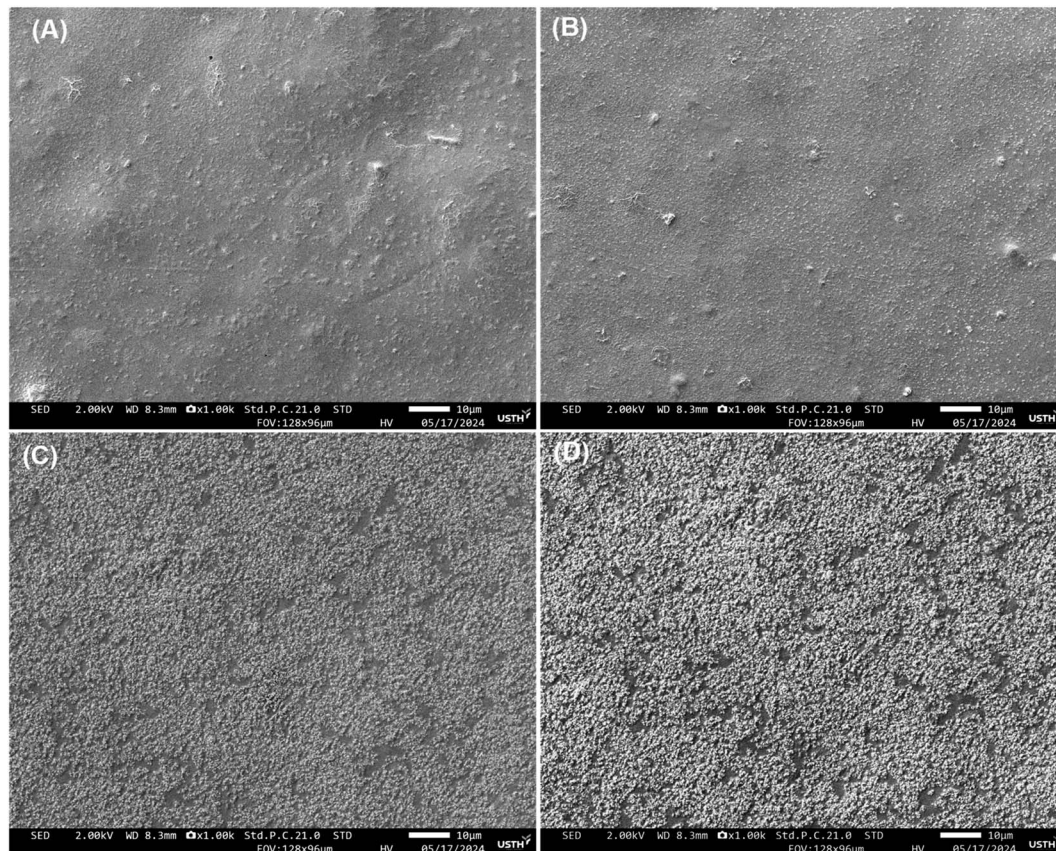


Fig. 2 SEM images of CS–CD/0.5% $\text{TiO}_2$  (A), CS–CD/1% $\text{TiO}_2$  (B), CS–CD/1.5% $\text{TiO}_2$  (C), and CS–CD/2% $\text{TiO}_2$  (D) films.



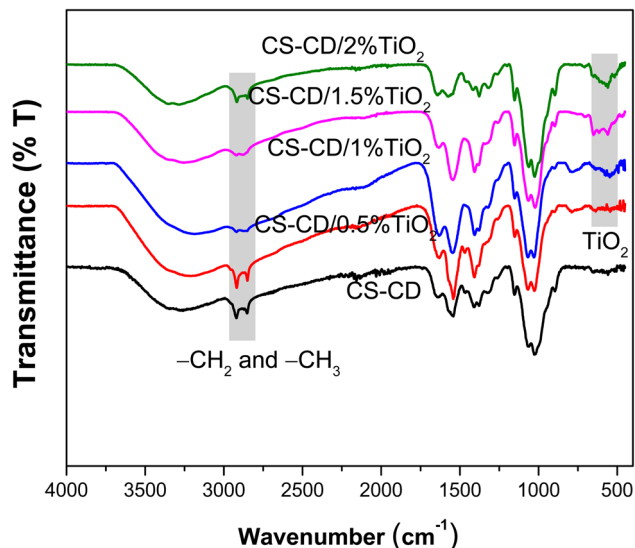


Fig. 3 FT-IR spectra of CS-CD and CS-CD/TiO<sub>2</sub> films.

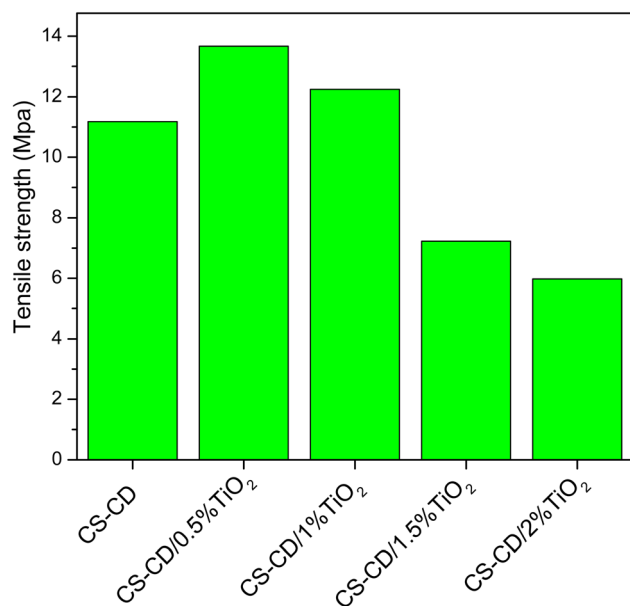


Fig. 4 Tensile strength of CS-CD and CS-CD/TiO<sub>2</sub> films.

Fourier-transform infrared spectroscopy (FTIR) was used to determine the functional groups present on the surface of the chitosan-cyclodextrin and CS-CD/TiO<sub>2</sub> films. In Fig. 3, chitosan-cyclodextrin (CS-CD) and CS-CD/TiO<sub>2</sub> exhibit vibrations in the range of 3200 to 3400 cm<sup>-1</sup>, which are assigned to the stretching vibrations of -OH and -NH<sub>2</sub> groups.<sup>38</sup> Vibrations in the range of 2881 to 2928 cm<sup>-1</sup> are assigned to the stretching vibrations of -CH<sub>2</sub> and -CH<sub>3</sub> groups, as well as the bending vibrations of the -NH groups (1636 cm<sup>-1</sup>), symmetric deformation vibrations of -CH<sub>3</sub> (1405 cm<sup>-1</sup>), bands at 1640, 1560 and 1328 cm<sup>-1</sup> assigned to the amide bond in the acylated units of CS, and stretching vibrations of C-O-C (1026 cm<sup>-1</sup>) typical for CD and CS.<sup>39</sup> Minor changes in the area of the stretching vibrations of C-O-C upon increasing concentration of TiO<sub>2</sub> NPs indicate insignificant interactions between titanium dioxide and carbohydrates. In addition to the vibrations of the chitosan-cyclodextrin, CS-CD/TiO<sub>2</sub> films also exhibit vibrations in the range of 680–520 cm<sup>-1</sup>, which are assigned to the Ti-O bond, and these vibrations increase as the TiO<sub>2</sub> content in the CS-CD/TiO<sub>2</sub> films increases. Obtained results are in a good agreement with previously published data concerning FTIR analysis of CS-TiO<sub>2</sub> NPs but here we have in the first time demonstrated it for the triple composite CS-CD/TiO<sub>2</sub>.<sup>40</sup>

The thickness of the films is equivalent to a thickness of (30–40 μm) used to measure tensile strength. All CS-CD and CS-CD/TiO<sub>2</sub> films are reviewed through tensile strength. Fig. 4 confirms that the content of TiO<sub>2</sub> nanoparticles significantly affects the tensile strength of CS-CD films, with an increase in TiO<sub>2</sub> content in the range of 0.5 to 1% wt resulting in a slight increase in tensile strength from 11.18 to 12.25%. The increase in mechanical properties is due to the increased interaction of cross-linking and surface interaction between CS-CD and TiO<sub>2</sub>. This result is consistent with the reports of Zhang<sup>27</sup> and Balasubramanian.<sup>41</sup> However, when the TiO<sub>2</sub> content exceeds 1% wt to 1.5 and 2.0% wt, the tensile strength decreases sharply to 7.23 and 5.98 MPa, respectively, due to the limited interaction between CS-CD and TiO<sub>2</sub>, related to phase separation using synthetic fillers in the polymer matrix.<sup>42</sup>

### 3.3. The antibacterial ability of the coatings

CS-CD/TiO<sub>2</sub> coatings are used to evaluate the antibacterial ability against Gram-negative bacteria (*Escherichia coli*) and Gram-positive bacteria (*Staphylococcus aureus*) as presented in

Table 1 Results of evaluating the antibacterial ability against *E. coli* and *S. aureus* of CS-CD/TiO<sub>2</sub> coatings<sup>a</sup>

Sample symbol	Sample	Concentration of <i>E. coli</i> after 15 min of exposure, CFU mL <sup>-1</sup>	Concentration of <i>S. aureus</i> after 15 min of exposure, CFU mL <sup>-1</sup>
X0 (control)	—	1.23 × 10 <sup>3</sup>	2.41 × 10 <sup>3</sup>
X1	CS-CD	7.40 × 10 <sup>1</sup>	2.01 × 10 <sup>1</sup>
X2	CS-CD/0.5%TiO <sub>2</sub>	6.65 × 10 <sup>1</sup>	1.21 × 10 <sup>1</sup>
X3	CS-CD/1.0%TiO <sub>2</sub>	4.60 × 10 <sup>1</sup>	1.22 × 10 <sup>1</sup>
X4	CS-CD/1.5%TiO <sub>2</sub>	5.20 × 10 <sup>1</sup>	1.49 × 10 <sup>1</sup>
X5	CS-CD/2.0%TiO <sub>2</sub>	2.50 × 10 <sup>1</sup>	1.32 × 10 <sup>1</sup>

<sup>a</sup> Therefore, the CS-CD/0.5%TiO<sub>2</sub> and CS-CD/1.0%TiO<sub>2</sub> films have improved antibacterial and mechanical properties compared to the CS-CD membrane and were chosen for testing the preservation of avocados.



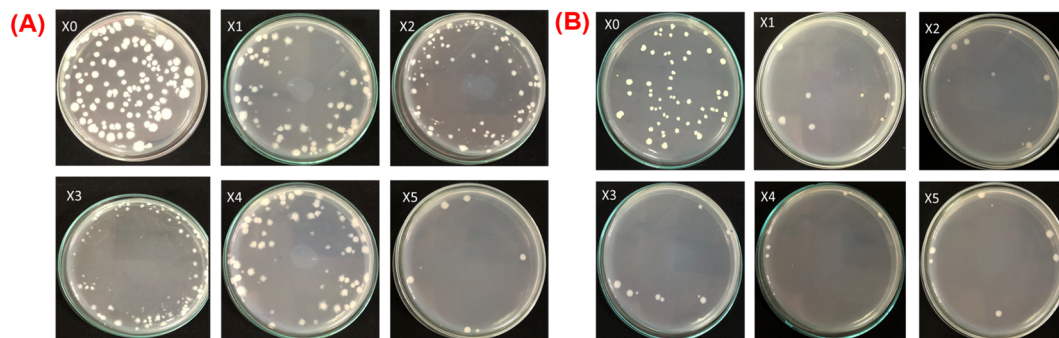


Fig. 5 Images of experimental Petri dishes containing colonies for *E. coli* (A) and *S. aureus* (B).

Table 1 and Fig. 5. Table 1 confirms that CS-CD/TiO<sub>2</sub> coatings have the ability to resist both Gram-negative and Gram-positive bacteria. The CS-CD/2%TiO<sub>2</sub> sample with the highest TiO<sub>2</sub> content (sample X5) shows the highest antibacterial ability against *E. coli*, while the CS-CD/TiO<sub>2</sub> films containing 0.5 to 1%

wt demonstrate the highest antibacterial ability against *S. aureus*. The CS-CD/TiO<sub>2</sub> films exhibit better antibacterial ability than the CS-CD film, as under light conditions, the TiO<sub>2</sub> component can be activated by light to form reactive oxygen



Fig. 6 Images of avocados coated with CS-CD/0.5%TiO<sub>2</sub> and CS-CD/1.0%TiO<sub>2</sub> and control samples.



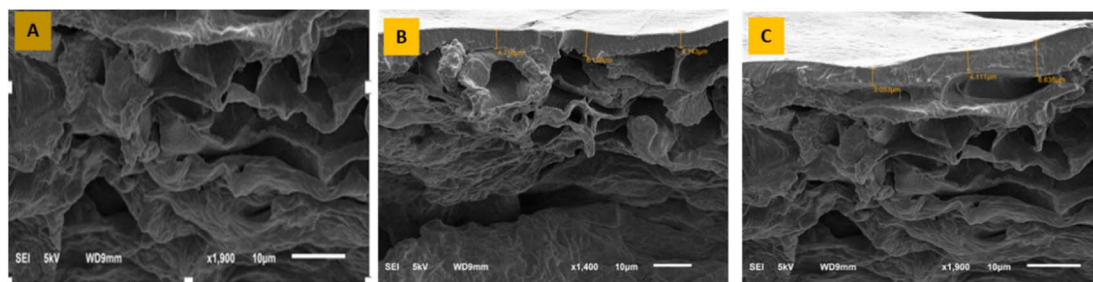


Fig. 7 SEM images of avocado peel (A); coated by CS-CD/0.5%TiO<sub>2</sub> (B) and CS-CD/1.0%TiO<sub>2</sub> (C) formulas.

species such as hydroxyl and superoxide radicals, which can inhibit or destroy bacteria.<sup>20,21,24</sup>

### 3.4. Testing the ability to preserve avocados of CS/CD-TiO<sub>2</sub> NPs coatings

**3.4.1 Sensory evaluation.** Fig. 6 showed the changes of avocado samples during 7 days of storage under the experimental conditions of 30 °C and 80% relative humidity, and in the air. In Fig. 6, all avocado samples did not show any changes after 1 day of storage. However, by the 4 days, the avocados not covered with the ultra-thin CS-CS/TiO<sub>2</sub> films began to develop dark spots and rot at the head of the fruit. The samples covered by CS-CD/0.5%TiO<sub>2</sub> and CS-CD/1.0%TiO<sub>2</sub> products both demonstrated significant avocado preservation effectiveness. In particular, the avocados covered by the CS-CD/1.0%TiO<sub>2</sub> film did not rot after 7 days of storage and were even riper compared to the avocados preserved with the CS-CD/1.0%TiO<sub>2</sub> film.

Fig. 7 presented the SEM images of cross-sectional views of avocado peel and avocado samples coated with CS-CD/0.5%TiO<sub>2</sub> and CS-CD/1.0%TiO<sub>2</sub> formulas. It can be seen that, the surface morphology of the avocado peel (Fig. 7A) was relatively rough, with cracks and grooves on the outer surface. When coated with CS-CD/0.5%TiO<sub>2</sub> and CS-CD/1.0%TiO<sub>2</sub> formulas (Fig. 7B and C), the avocado peel layers become relatively smooth, uniform without cracks, and with a relatively thickness

in the range of 3–6 µm. In our previous study, the coating thickness on avocado was about 23 µm, although in both cases the chitosan solution used had a concentration of 1.5%.<sup>32</sup> This can be explained by the fact that the avocado varieties used in two studies were different. The avocado is the *Persea americana* Mill variety, with a relatively smooth exterior.<sup>32</sup>

**3.4.2 Mass loss.** Different types of fruits tend to lose weight as water moves from the inside to the surface, leading to water evaporating into the air during storage. The mass model of an avocado during storage is presented in Fig. 8. Fig. 8 shows the decrease in weight of the avocado after periods of storage. Prolonged storage can increase respiration time, leading to water evaporation and significant nutrient loss. CS-CD/TiO<sub>2</sub> films have the ability to significantly prevent weight loss due to water loss. Therefore, CS-CD/TiO<sub>2</sub> films have been proven to reduce water loss, with the membrane layers acting as more effective moisture barrier fences.<sup>13</sup> Thus, the combined use of CS-CD and TiO<sub>2</sub> has a synergistic effect in fruit preservation.<sup>43</sup>

**3.4.3 Hardness.** Fig. 9 shows the hardness of the avocado tends to decrease to 0, the reason being that when the fruit ripens, the hardness decreases. With the samples preserved with CS-CD/0.5%TiO<sub>2</sub> and CS-CS/1%TiO<sub>2</sub> films, the hardness decreases slightly and evenly, indicating good and effective preservation films that inhibit the ripening process of the fruit. The hardness of an avocado decreases due to the conversion of

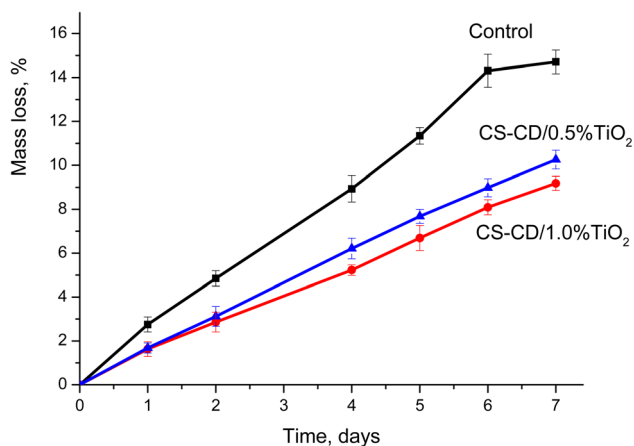


Fig. 8 Mass loss of avocado samples coated by CS-CD/0.5%TiO<sub>2</sub> and CS-CD/1.0%TiO<sub>2</sub> compared to control sample.

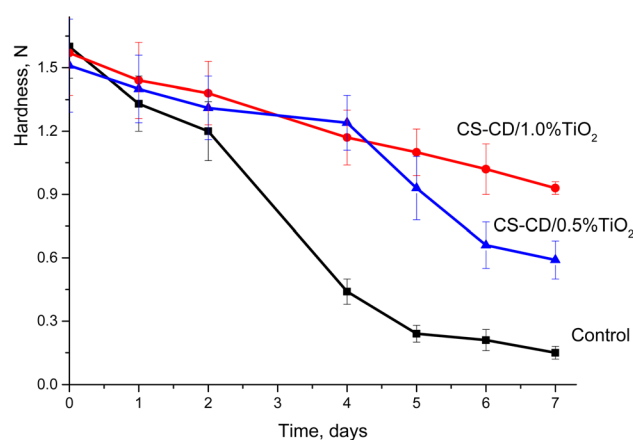


Fig. 9 The hardness change of avocados coated by CS-CD/0.5%TiO<sub>2</sub> and CS-CD/1.0%TiO<sub>2</sub> compared to control samples.



protopectin and starch into pectin, sugar and limiting the water loss process, resulting in a softer avocado.<sup>32</sup>

## 4 Conclusion

In summary, TiO<sub>2</sub> nanomaterial with a surface area of 109 m<sup>2</sup> g<sup>-1</sup>, nanoparticle size of about 10–20 nm, synthesized quickly by the supported-microwave hydrothermal method has been used as an antibacterial additive in the CS-CD/TiO<sub>2</sub>NPs films. The chitosan/TiO<sub>2</sub> films combined with cyclodextrin enhances antibacterial activity and significantly improves the mechanical properties of the polymer film. The CS-CD/1.0%TiO<sub>2</sub>NPs film coated on the avocado surface is relatively uniform and smooth, with no cracks observed on the surface. The CS-CD/TiO<sub>2</sub>NPs film with 1.0% of TiO<sub>2</sub> content shows high effectiveness in extending the freshness and shelf life of avocados under conditions of 30 °C and 80% relative humidity. Furthermore, the CS-CD/TiO<sub>2</sub>NPs film is effective against Gram-negative bacteria (*Escherichia coli*) and Gram-positive bacteria (*Staphylococcus aureus*) achieving over 99.5% after 15 min of contact. The content of TiO<sub>2</sub> nanoparticles in CS/CD-TiO<sub>2</sub>NP also affects the tensile strength, antibacterial activity, ripening rate, ethylene production rate, and water vapor permeability in the food preservation process of the CS-CD file. The results show that the edible, biocompatible CS-CD/TiO<sub>2</sub>NPs file with the ability to biodegrade holds promise as a coating for preserving avocados and other foods to replace petroleum-derived toxic films that pose risks to human health.

## Data availability

The authors confirm that the data supporting the findings of this study are available within the article.

## Author contributions

Thi Lan Pham: conceptualization, methodology, writing – original draft, investigation, writing – review & editing; Manh B Nguyen: investigation, writing – original draft; Van Cuong Bui: investigation, validation, formal analysis; Thi Xuyen Nguyen: investigation; Savitskaya T. A.: formal analysis, visualization; Irina Le-Deygen: validation, formal analysis. Hoang Thai: writing – review & editing; Dai Lam Tran: conceptualization, supervision.

## Conflicts of interest

The authors declare that they have no known competing financial interests or personal relationships that could have appeared to influence the work reported in this paper.

## Acknowledgements

This work was funded by The Vietnam Ministry of Science and Technology (MOST) under the grant number NDT/BY/22/01.

## References

- 1 B. Abera, R. Duraisamy and T. Birhanu, *J. Agric. Food Res.*, 2024, **15**, 100916.
- 2 T. Sharma, G. Kaur, A. Singh, V. Kumar and B. N. Dar, *Sci. Hortic.*, 2024, **332**, 113239.
- 3 M. Y. Khalid and Z. U. Arif, *Food Packag. Shelf Life*, 2022, **33**, 100892.
- 4 M. B. Nguyen, H. V Doan, D. Le, H. Tan and T. Dai, *J. Environ. Chem. Eng.*, 2024, **12**, 112965.
- 5 R. Saberi, M. Vatankhah, M. Hassanisaadi, Z. Shafiehematabad and J. F. Kennedy, *Int. J. Biol. Macromol.*, 2024, **254**, 127677.
- 6 Z. Zhang, Q. Jiang, G. Yang, X. Zhang, X. Jiang, B. He and J. Chen, *Ind. Crops Prod.*, 2023, **205**, 117430.
- 7 C. Bhan, R. Asrey, N. Kumar, S. Gaur, G. Chawla, R. Kumar and R. Kumar, *Int. J. Biol. Macromol.*, 2022, **222**, 2922–2935.
- 8 M. Barik, G. V. S. Bhagyaraj, K. Kumar and R. Shams, *J. Agric. Food Res.*, 2024, **16**, 101164.
- 9 M. H. Wardak, F. N. Nkede, T. T. Van, F. Meng, F. Tanaka and F. Tanaka, *Prog. Org. Coat.*, 2024, **187**, 108127.
- 10 L. Cheng, X. Li, S. An, Z. Liu, Y. Liu and D. Ren, *Food Packag. Shelf Life*, 2024, **43**, 101295.
- 11 H. Rohasmizah and M. Azizah, *Appl. Food Res.*, 2022, **2**, 100221.
- 12 L. Motelica, D. Ficai, A. Ficai, O. C. Oprea, D. A. Kaya and E. Andronescu, *Foods*, 2020, **9**(10), 1438.
- 13 Y. Li, L. Zheng, G. Mustafa, Z. Shao, H. Liu, Y. Li, Y. Wang, L. Liu, C. Xu, T. Wang, J. Zheng, F. Meng and Q. Wang, *Food Chem.*, 2024, **454**, 139685.
- 14 B. Fu, S. Mei, X. Su, H. Chen, J. Zhu, Z. Zheng, H. Lin, C. Dai, R. Luque and D. Yang, *Int. J. Biol. Macromol.*, 2021, **191**, 1164–1174.
- 15 G. Ghoshal and J. Singh, *Food Chem. Adv.*, 2024, **4**, 100651.
- 16 L. Motelica, D. Ficai, A. Ficai, C. Ilie, O. Oprea and E. Andronescu, *Foods*, 2020, **9**(12), 1801.
- 17 M. B. Nguyen, P. T. Lan, N. T. Anh, N. N. Tung, S. Guan, V. P. Ting, T. T. B. Nguyen, H. V. Doan, M. T. Tung and T. D. Lam, *RSC Adv.*, 2023, **13**, 35339–35348.
- 18 F. Leonardo, G. De Menezes, R. Henrique, D. L. Leite, F. Klebson, A. Indrat, E. Maria and M. Aroucha, *Food Chem.*, 2024, **433**, 137387.
- 19 H. S. Tohamy, S. A. A. Mohamed, M. El-sakhawy, M. Elsayed and S. Kamel, *Int. J. Biol. Macromol.*, 2024, **257**, 128589.
- 20 M. Hussain, S. Bensaid, F. Geobaldo, G. Saracco and N. Russo, *Ind. Eng. Chem. Res.*, 2011, 2536–2543.
- 21 S. Agrarie and V. A. I, *Biosyst. Eng.*, 2015, **132**, 61–70.
- 22 V. K. Yemmireddy and Y. Hung, *Food Control*, 2015, **57**, 82–88.
- 23 M. Wang, Z. Xu, Z. Qi, Y. Cai, G. Li, W. Choi and T. An, *Chem. Eng. J.*, 2023, **468**, 143680.
- 24 M. Cho, Y. Choi, H. Park, K. Kim, G. J. Woo and J. Park, *J. Food Prot.*, 2007, **70**, 97–101.
- 25 Y. Xing, H. Yang, X. Guo, X. Bi, X. Liu, Q. Xu, Q. Wang, W. Li, X. Li, Y. Shui, C. Chen and Y. Zheng, *Sci. Hortic.*, 2020, **263**, 109135.



- 26 A. Spoială, C. I. Ilie, G. Dolete, A. M. Croitoru, V. A. Surdu, R. D. Truşcă, L. Motelica, O. C. Oprea, D. Ficăi, A. Ficăi, E. Andronescu and L. M. Diţu, *Membranes*, 2022, **12**(8), 804.
- 27 X. Zhang, G. Xiao, Y. Wang, Y. Zhao, H. Su and T. Tan, *Carbohydr. Polym.*, 2017, **169**, 101–107.
- 28 H. Du, T. Min, X. Sun, X. Bian, Z. Zhu and Y. Wen, *Food Biosci.*, 2022, **50**, 102168.
- 29 I. Zarandona, C. Barba, P. Guerrero, K. De Caba and J. Mat, *Food Hydrocolloids*, 2020, **104**, 105720.
- 30 M. Petitjean, I. X. García, Z. José and R. Isasi, *Environ. Chem. Lett.*, 2021, **19**, 3465–3476.
- 31 A. Cid-samamed, J. Rakmai, J. Carlos, J. Simal-gandara and G. Astray, *Food Chem.*, 2022, **384**, 132467.
- 32 T. L. Pham, V. C. Bui, H. K. Le, T. M. H. Le, X. M. Vu, T. A. Nguyen, T. T. H. Pham, T. T. Mai, T. A. Savitskaya and D. L. Tran, *J. Coat. Technol. Res.*, 2024, DOI: [10.1007/s11998-024-00919-2](https://doi.org/10.1007/s11998-024-00919-2).
- 33 M. B. Nguyen, L. H. T. Nguyen, M. T. Le, N. Q. Tran, N. H. T. Tran, P. H. Tran, A. T. T. Pham, L. D. Tran and T. L. H. Doan, *J. Ind. Eng. Chem.*, 2024, **134**, 217–230.
- 34 A. A. Silahua-Pavón, C. G. Espinosa-González, F. Ortiz-Chi, J. G. Pacheco-Sosa, H. Pérez-Vidal, J. C. Arévalo-Pérez, S. Godavarthi and J. G. Torres-Torres, *Catal. Commun.*, 2019, **129**, 105723.
- 35 S. Bibi, S. S. Shah, F. Muhammad, M. Siddiq, L. Kiran, S. A. Aldossari, M. Sheikh Saleh Mushab and S. Sarwar, *Chemosphere*, 2023, **339**, 139583.
- 36 Y. Li, T. E. L. Liu, S. Yang, J. Qian and Z. Ma, *J. Mater. Sci.*, 2020, **55**, 670–679.
- 37 L. Li, C. Eng, R. J. Desnick, J. German and N. A. Ellis, *Mol. Genet. Metab.*, 1998, **64**, 286–290.
- 38 S. Iswarya, T. Theivasanthi and S. C. B. Gopinath, *Colloids Surf., A*, 2024, **693**, 134018.
- 39 A. El-araby, W. Janati, R. Ullah, N. Uddin and A. Bari, *Heliyon*, 2024, **10**, e29286.
- 40 Y. Xing, X. Li, X. Guo, W. Li, J. Chen, Q. Liu, Q. Xu, Q. Wang, H. Yang, Y. Shui and X. Bi, *Nanomaterials*, 2020, **10**, 1–19.
- 41 R. Balasubramanian, S. S. Kim, J. Lee and J. Lee, *Int. J. Biol. Macromol.*, 2019, **123**, 1020–1027.
- 42 S. Roy, L. Zhai, H. C. Kim, D. H. Pham, H. Alrobei and J. Kim, *Polymers*, 2021, **13**, 1–18.
- 43 S. Mallakpour, F. Sirous and C. Mustansar, *Int. J. Biol. Macromol.*, 2021, **170**, 701–716.

